

Letter

Generation of 8.3 dB continuous variable quantum entanglement at a telecommunication wavelength of 1550 nm

Feng Jinxia^{1,2}, Wan Zhenju¹, Li Yuanji^{1,2} and Zhang Kuanshou^{1,2}¹ State Key Laboratory of Quantum Optics and Quantum Optics Devices, Institute of Opto-Electronics, Shanxi University, Taiyuan 030006, People's Republic of China² Collaborative Innovation Centre of Extreme Optics, Shanxi University, Taiyuan, Shanxi 030006, People's Republic of ChinaE-mail: kuanshou@sxu.edu.cn

Received 21 April 2017

Accepted for publication 26 October 2017

Published 18 December 2017

**Abstract**

Continuous variable quantum entanglement at a telecommunication wavelength of 1550 nm is experimentally generated using a single nondegenerate optical parametric amplifier based on a type-II periodically poled KTiOPO₄ crystal. The triply resonant of the nondegenerate optical parametric amplifier is adjusted by tuning the crystal temperature and tilting the orientation of the crystal in the optical cavity. Einstein–Podolsky–Rosen-entangled beams with quantum correlations of 8.3 dB for both the amplitude and phase quadratures are experimentally generated. This system can be used for continuous variable fibre-based quantum communication.

Keywords: quantum entanglement, continuous variable, telecommunication wavelength, nondegenerate optical parametric amplifier

(Some figures may appear in colour only in the online journal)

1. Introduction

Continuous variable (CV) quantum entanglement is a fundamental resource for CV quantum communication and quantum computation [1, 2]. It is useful for a wide variety of applications, including quantum teleportation, quantum dense coding, quantum key distribution (QKD), and high-precision quantum measurement [3–10]. A pair of CV entangled beams has been generated using a subthreshold nondegenerate optical parametric amplifier (NOPA) and demonstrated the Einstein–Podolsky–Rosen (EPR) paradox for the first time in the CV regime [11]. Later, bright quantum entanglement with anticorrelated amplitude (phase) and correlated phase (amplitude) was observed from a NOPA with an injected signal operating at deamplification (amplification) [12–14]. Recently, 8.4 dB CV quantum entanglement at 1080 nm was experimentally generated using a single NOPA with a wedged type-II KTP crystal [15].

For practical applications of CV quantum information, it is crucial to achieve CV quantum entangled states with high entanglement and compact configurations. The non-classical properties of the light emitted by a NOPA can be enhanced by making the pump power as close as possible to the oscillation threshold. The triply resonance of the NOPA with the signal, idler and pump modes simultaneously resonating inside the cavity allows a lower threshold [16], and a high-quality non-classical state can be obtained using this type of device with a relatively low pump power. In particular, the low threshold is useful for CV quantum networks in which multipartite entangled states are required [17, 18]. To realise the triply resonant condition in an optical cavity, the temperature of the nonlinear crystal should first be controlled. An extra optical element was inserted in the cavity to compensate the dispersion of the optical modes [19, 20], but the inserted element increased the intracavity loss. A wedged nonlinear crystal was used to

compensate the dispersion by adjusting the crystal interaction length [15, 21]. The triply resonance condition can also be realised using a convenient method to tilt the orientation of the crystal in the optical cavity without a special crystal wedge cutting [22]. However, to achieve the triply resonant condition, it is necessary to control the nonlinear crystal temperature with an excellent temperature controller and fulfil strict constraints on the optical and geometrical properties of the optical cavity. In another hand, it is necessary to achieve CV quantum entanglement at the telecommunication wavelength of 1550 nm because the optical power attenuation of light in standard telecommunication fibres is lowest at 1550 nm. The EPR-entangled state at 1550 nm has been generated via interference of two single-mode squeezed vacuum states on a 50R/50T beam splitter from two degenerate optical parametric oscillators (OPOs) [23]. Obviously, using a single NOPA to generate quantum entanglement is relatively compact. Using quantum entanglement at 1550 nm, CV quantum communication based on standard fibres becomes feasible.

In this paper, we construct a low-threshold triply resonant OPO with a type-II periodically poled potassium titanyl phosphate (PPKTP) crystal. And CV quantum entanglement at the telecommunication wavelength of 1550 nm is generated using a triply resonant NOPA at a pump power below the threshold.

2. Experimental setup

The schematic of the experimental setup used to generate the CV quantum entanglement is shown in figure 1. A commercial fibre laser (NP Photonic Inc.) provided an output power of 2.0 W with continuous-wave (CW) single-frequency operation at 1550 nm. An optical isolator (OI) was used to eliminate the back-reflexion light. A half-wave plate (HWP1) was used to control the laser beam polarisation. The laser beam was sent through a mode cleaner (MC1) with a finesse of 500 and linewidth of 600 kHz for preliminary filtering of the laser spatial mode and excess intensity noise. An electro-optical modulator (EOM) driven by a radio frequency of 65 MHz was employed to lock the MC1 cavity using the Pound–Drever–Hall (PDH) technique [24]. The output from MC1 was split by a partial reflexion mirror (PRM). The main portion was injected into an external enhanced second-harmonic generation (SHG) cavity to obtain a high-power, low-noise CW laser with a wavelength of 775 nm that acted as the pump of the NOPA. The residual portion was used as the injected signal light of the NOPA. The external enhanced SHG cavity was composed of a linear cavity and a periodically poled LiNbO₃ crystal. A 1 W single-frequency laser at 775 nm was obtained with the frequency doubling efficiency of 85%. MC2, with a linewidth of 600 kHz, and MC3, with a linewidth of 700 kHz, were used to further reduce the excess intensity noises of the injected signal and pump of the NOPA, respectively. MC2 and MC3 were also locked using the PDH technique with radio frequencies of 65 and 82 MHz, respectively. The power transmittances of the three MCs were approximately 80%. Using the MCs, the intensity noises of the pump and injected signal of the NOPA reached the shot noise level (SNL) for analysis frequencies higher than 4 MHz.

The NOPA was composed of two concave mirrors with radii of 30 mm and a type-II PPKTP crystal with dimensions of $1 \times 2 \times 10 \text{ mm}^3$. Both end faces of PPKTP were antireflexion coated for wavelengths of 1550 nm ($R_{1550 \text{ nm}} < 0.1\%$) and 775 nm ($R_{775 \text{ nm}} < 0.25\%$). The input coupler of the NOPA provided partial transmission (PT) at 775 nm ($T_{775 \text{ nm}} = 10.0\%$) and high reflexion (HR) at 1550 nm ($R_{1550 \text{ nm}} > 99.9\%$). The output coupler provided PT at 1550 nm ($T_{1550 \text{ nm}} = 6.8\%$) and HR at 775 nm ($R_{775 \text{ nm}} > 99.7\%$). The geometric length of the NOPA cavity was 65 mm, resulting in a cavity waist of 61 μm for the injected signal at 1550 nm. The measured finesse of the NOPA for the injected signal was 90. It can be calculated that the cavity linewidth was 25 MHz, the intracavity loss was $\Delta = 0.18\%$, and the signal escape efficiency from the NOPA was $\eta_{\text{esc}} = T/(T + \Delta) = 97.4\%$. The measured finesse of the NOPA for the pump was 58.

The PPKTP crystal temperature was controlled using a home-made temperature controller with an accuracy of 0.003 °C. The orientation of crystal could be finely adjusted using a 5D adjusting frame with an accuracy of 1 μm for translation and 0.1 mrad for rotation. In our experiment, the triply resonant condition of the NOPA was realised by precisely controlling the crystal temperature and by fine tilting of the orientation angle of the crystal. Because the tilting angle of PPKTP was very fine, the mode and phase mismatching could be negligible. The injected signal was also used to align the cavity and measure the classical gain of the NOPA.

When the relative phase between the pump and injected signal was locked to π using a piezo-electric transducer (PZT1) mounted on an HR mirror, the NOPA was operated in a state of deamplification. Bright EPR-entangled beams with correlated amplitude quadratures and phase quadratures were produced from the NOPA. EPR-entangled beams with frequencies that were identical to that of the injected signal and polarised orthogonally to each other, were separated using a polarising beam splitter (PBS1). The quantum correlation between the amplitude quadratures and phase quadratures of the EPR-entangled beams was measured using a two-mode homodyne detector for CV quantum entanglement [25] composed of PBS2, PBS3, HWP4, a pair of high-quantum-efficiency InGaAs photo detectors (PD1 and PD2, HAMAMATSU Photonics K. K., G10899) and two radio frequency power splitters (RFs). The EPR beams were combined by PBS2, and the relative phase between two EPR beams was locked to $\pi/2$ using PZT3 mounted on an HR mirror. The output two beams from a 50R/50T beam splitter consisting of HWP4 and PBS3 were detected by PD1 and PD2. The output photo-currents from RFs were combined by the positive and the negative power combiner (\oplus , \ominus) to obtain the noise powers of the amplitude sum and phase difference, respectively. They were then measured using a spectrum analyser (SA). This type of detection system for bright EPR beams with anticorrelated amplitude quadratures and correlated phase quadratures has the advantage that a local oscillator (LO) is not required and random phase variations between the measured quantum state and LO need not be considered.

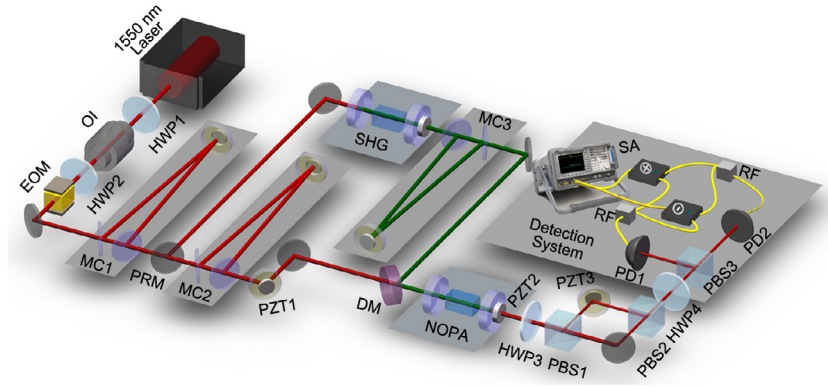


Figure 1. Schematic of the experimental setup used to generate CV quantum entanglement. HWP1-4: half-wave plate; EOM: electro-optic modulator; SHG: second harmonic generator; MC1-2: mode cleaner of 1550 nm; MC3: mode cleaner of 775 nm; PRM: partial reflexion mirror; DM: dichroic mirror; PZT1-3: piezo-electric transducer; PBS1-3: polarising beam splitter; SA: spectrum analyser; PD1-2: photo detector; RF: radio frequency power splitter; \oplus : positive power combiner; \ominus : negative power combiner; NOPA: nondegenerate optical parametric amplifier.

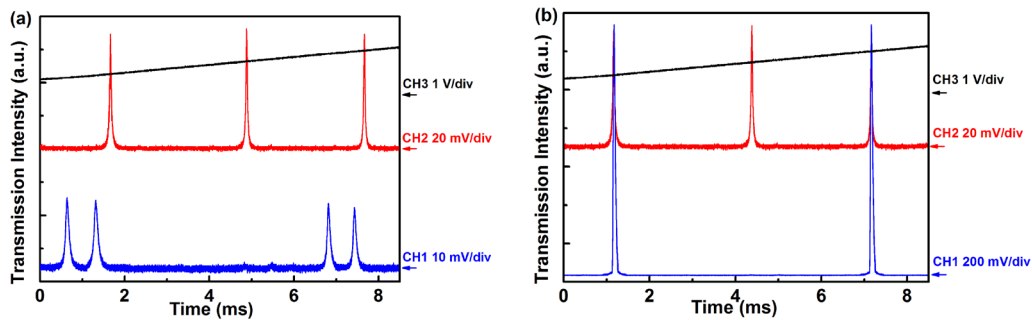


Figure 2. Transmission intensity of the pump and injected signal when the length of the NOPA was scanned. (a) The s_e , s_o and pump modes were not in resonance. (b) The s_e , s_o and pump modes were in resonance due to the fine-tuning of the temperature and tilting angle of the PPKTP crystal. The black line is the 1% monitoring signal of DC voltage; the red and blue curves are the transmission intensity of the pump and injected signal, respectively.

3. Experimental results

The realization of the triply resonant condition of the NOPA is shown in figure 2. The length of the NOPA cavity was scanned by tuning the DC voltage on PZT2. The black line in figure 2 is the 1% monitoring signal of the DC voltage. The red and blue curves indicate the transmission intensities of the pump and injected signal, respectively. When the polarisation of the injected signal incidence to the PPKTP was set to an angle of 45° , the modes polarised along the slow and fast axes (s_e mode and s_o mode) corresponded to the signal and idler of the NOPA, respectively. Figure 2(a) shows the transmission intensity of the s_e , s_o and pump modes; it is obvious that they are not in the resonance. First, by tuning the temperature of the PPKTP crystal to 34.5°C , the double resonance of the s_e and s_o mode was realised. Then, by fine-tuning the tilting angle of the PPKTP crystal by approximately 3 mrad to compensate the dispersion of the injected signal and pump, the triple resonance was realised, as shown in figure 2(b). For the OPO in triply resonant oscillation, the measured threshold was 46 mW.

When the pump power was 40 mW, which is below the OPO threshold, and the injected signal power was 10 mW, a classical gain of the NOPA of 40 times was observed, as shown in figure 2(b). It should be noted that the actual injected

signal power in the NOPA cavity is very small because the injected signal was coupled into the cavity through the input coupler with HR at 1550 nm ($R_{1550\text{ nm}} > 99.9\%$). When the relative phase between the pump and injected signal was locked to π and the NOPA was operated in the state of deamplification, a mean field output power of $680\ \mu\text{W}$ from the NOPA was obtained. The noise powers of the amplitude sum and the phase difference of the NOPA output beams were measured using an SA, as shown in figure 3. The spectrum analysis parameters were as follows: Fourier analysis frequency of 7 MHz in the zero span mode, resolution bandwidth (RBW) of 30 kHz, and video bandwidth (VBW) of 300 Hz. The curves (i) in figure 3 are the SNL corresponding to the noise power of a $680\ \mu\text{W}$ coherent state that was achieved by adjusting the power of the injected signal of the NOPA without the pump. The curves (ii) in figures 3(a) and (b) are the measured correlation variances of the amplitude sum $\langle\langle\delta^2(\hat{X}_a + \hat{X}_b)\rangle\rangle$ and phase difference $\langle\langle\delta^2(\hat{Y}_a - \hat{Y}_b)\rangle\rangle$ of the NOPA output beams. It can be seen that they are 8.44 ± 0.13 and 8.30 ± 0.11 dB below the corresponding SNLs. The bright EPR-entangled beams satisfy the criteria for inseparability [26]: $\langle\langle\delta^2(\hat{X}_a + \hat{X}_b)\rangle\rangle + \langle\langle\delta^2(\hat{Y}_a - \hat{Y}_b)\rangle\rangle = 0.291 < 2$, corresponding to the measured entanglement of 8.3 dB without

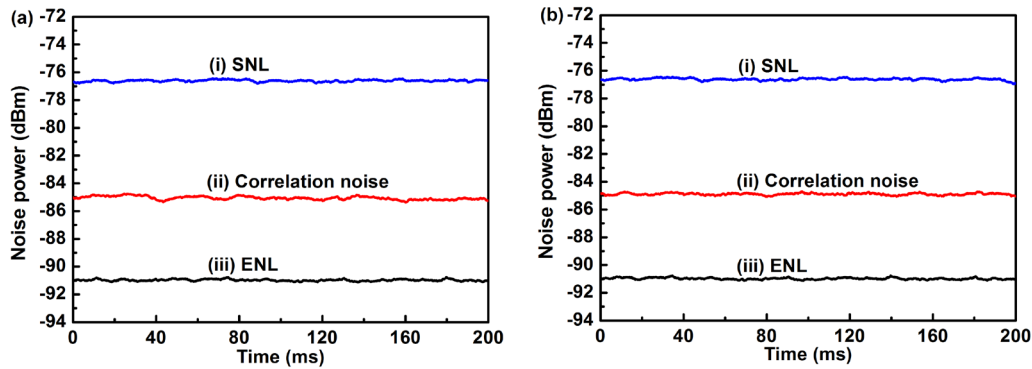


Figure 3. Measured noise powers of the EPR-entangled beams from the NOPA at analysis frequency of 7 MHz, where, (i) is the SNL, (ii) is the correlation variance of amplitude sum (a) and phase difference (b), and (iii) is the ENL. The SA measurement parameters are RBW 30 kHz and VBW 300 Hz.

the subtraction of the electronics noise. The curves (iii) are the electronics noise level (ENL) of the PDs that were 14 dB below the SNL.

The measured detection efficiency of the detection system was 95%. Taking into account the imperfect detection efficiency and the influence of ENL, the inferred quantum correlation of the bright EPR-entangled beams should be $\langle \delta^2(\hat{X}_a + \hat{X}_b) \rangle = 9.77 \pm 0.14$ dB and $\langle \delta^2(\hat{Y}_a - \hat{Y}_b) \rangle = 9.59 \pm 0.12$ dB below the SNL. Obviously, the experimental results can be further improved by increasing the detection efficiency and decreasing the ENL.

4. Conclusions

We have generated CV quantum entanglement at a telecommunication wavelength of 1550 nm using a single NOPA with a type-II PPKTP crystal. By controlling the PPKTP temperature using an excellent home-made temperature controller and fine-tilting the orientation of the PPKTP crystal, a triply resonant OPO with a low threshold of 46 mW was realised. EPR-entangled beams with quantum correlations of 8.3 dB for both the amplitude and phase quadratures were experimentally generated using a single NOPA at a pump power of 40 mW and the relative phase between the pump and injected signal was locked to π . The NOPA was operated in the state of deamplification with a mean field output power of 680 μ W. The generated CV quantum entanglement is highly suitable for demanding experiments, such as CV measurement-device-independence QKD based on standard fibres, owing to the fact that the tolerance of the excess noise in the quantum channel can be enhanced significantly if EPR-entangled beams are used. Additionally, the wavelength of 1550 nm makes the quantum states compatible with existing telecommunication fibre networks.

Acknowledgments

This research was supported by Key Project of the Ministry of Science and Technology of China (2016YFA0301401), and sponsored by the Fund for Shanxi “1331 Project” Key Subjects Construction (1331KS).

References

- [1] Kimble H J 2008 *Nature* **453** 1023–30
- [2] Braunstein S L and Loock P V 2005 *Rev. Mod. Phys.* **77** 513–77
- [3] Furusawa A, Sørensen J L, Braunstein S L, Fuchs C A, Kimble H J and Polzik E S 1998 *Science* **282** 706–9
- [4] Bouwmeester D, Pan J W, Mattle K, Eibl M, Weinfurter H and Zeilinger A 1997 *Nature* **390** 575–9
- [5] Li X Y, Pan Q, Jing J T, Zhang J, Xie C D and Peng K C 2002 *Phys. Rev. Lett.* **88** 047904
- [6] Jia X J, Su X L, Pan Q, Gao J R, Xie C D and Peng K C 2004 *Phys. Rev. Lett.* **93** 250503
- [7] Su X L, Hao S H, Deng X W, Ma L Y, Wang M H, Jia X J, Xie C D and Peng K C 2013 *Nat. Commun.* **4** 2828
- [8] Pirandola S, Ottaviani C, Spedalieri G, Weedbrook C, Braunstein S L, Lloyd S, Gehring T, Jacobsen C S and Andersen U L 2015 *Nat. Photon.* **9** 397–402
- [9] Sun H X, Liu K, Liu Z L, Guo P L, Zhang J X and Gao J R 2014 *Appl. Phys. Lett.* **104** 121908
- [10] Wang C, Wang T J and Zhang Y 2014 *Laser Phys. Lett.* **11** 065202
- [11] Ou Z Y, Pereira S P, Kimble H J and Peng K C 1992 *Phys. Rev. Lett.* **68** 3663
- [12] Zhang Y, Wang H, Li X Y, Jing J T, Xie C D and Peng K C 2000 *Phys. Rev. A* **62** 023813
- [13] Bowen W P, Schnabel R, Lam P K and Ralph T C 2003 *Phys. Rev. Lett.* **90** 043601
- [14] Laurat J, Coudreau T, Keller G, Treps N and Fabre C 2005 *Phys. Rev. A* **71** 022313
- [15] Zhou Y Y, Jia X J, Li F, Xie C D and Peng K C 2015 *Opt. Express* **23** 4952–9
- [16] Martinelli M, Zhang K S, Coudreau T, Maître A and Fabre C 2001 *J. Opt. A: Pure Appl. Opt.* **3** 300–3
- [17] Su X L, Tan A H, Jia X J, Zhang J, Xie C D and Peng K C 2007 *Phys. Rev. Lett.* **98** 070502
- [18] Yu Y B, Wang H J, Zhao J W, Ji F M and Wang Y J 2016 *Laser Phys. Lett.* **13** 085203
- [19] Mason E J and Wong N C 1998 *Opt. Lett.* **23** 1733–5
- [20] Croß P, Boller K J and Klein M E 2005 *Phys. Rev. A* **71** 043824
- [21] Imeshev G, Proctor M and Fejer M M 1998 *Opt. Lett.* **23** 165–7
- [22] D’Auria V, Fornaro S, Porzio A, Sete E A and Solimeno S 2008 *Appl. Phys. B* **91** 309–14
- [23] Eberle T, Handchen V and Schnabel R 2013 *Opt. Express* **21** 11546
- [24] Black Eric D 2001 *Am. J. Phys.* **69** 79–87
- [25] Zhang J and Peng K C 2000 *Phys. Rev. A* **62** 064302
- [26] Duan L M, Giedke G, Cirac J I and Zoller P 2000 *Phys. Rev. Lett.* **84** 2722–5